photonics

MDPI

Article

Efficient Trichromatic Nd:YLF Laser Emitting at 1047 nm, 1053 nm and 1314 nm

Felipe Maia Prado [1], Tomás Junqueira Franco [2] and Niklaus Ursus Wetter [1,*]

[1] Nuclear and Energy Research Institute, IPEN—CNEN, Av. Prof. Lineu Prestes 2242, São Paulo 05508-000, SP, Brazil; felipemp@usp.br
[2] Department of Physics, RWTH Aachen University, Templergraben 55, 52062 Aachen, Germany; tomas.franco@rwth-aachen.de
* Correspondence: nuwetter@ipen.br

Abstract: We report a Nd:YLF laser, side-pumped by a diode-stack at 797 nm with 1545 W peak power, resulting in triple-wavelength emission at 1314 nm, 1053 nm, and 1047 nm. The resonator is capable of emitting each wavelength separately as well as any combination of them simply by cavity alignment. When operating at 1314 nm, the laser reached record optical-to-optical efficiency of 49%, with a slope efficiency of 53%.

Keywords: Nd:YLF; solid-state Laser; multichromatic emission; trichromatic laser; triple-wavelength; 1314 nm; 1053 nm; 1047 nm

1. Introduction

Nd-doped crystals have demonstrated simultaneous laser emissions at different wavelengths, a property known as multichromatic emission. This can be observed for 1053 nm and 1047 nm emission from a Nd:YLF laser, or more distant emissions, such as 1064 nm and 1342 nm or 1064 nm and 946 nm for Nd:YAG lasers [1,2]. One of the remarkable features of multichromatic lasers is their ability to access multiple absorption lines of various materials. One notable application in this regard is Laser-Induced Breakdown Spectroscopy (LIBS). In this process, a short-to-ultrashort laser pulse turns a tiny fraction of a material sample into plasma for spectral analysis, thus avoiding extensive sample preparation. This technology can be used for several processes, including environmental monitoring through rapid analysis of air, soil sewage sludge, and wastewater, material analysis in the metal industry, and in mining as a tool for establishing ore composition [3].

Multichromatic lasers can also be applied in coating inspection [4], depth-resolved measurement of element composition [5], and microwave and terahertz generation [6,7]. Additionally, the frequency of the emitted beams can be doubled or tripled through second and third harmonic generation (SHG and THG), leading to green, red, and blue emissions that are interesting for applications in Light Detection and Ranging (LIDAR) and range finding [2,8,9]. These emissions can be Raman shifted before frequency double, leading to interesting medical applications such as retinal photocoagulation [10,11].

Amongst Neodymium (Nd)-doped crystals, which are well known for their 1 µm emissions, Yttrium Aluminum Garnet (Nd:YAG) and Yttrium Orthovanadate (Nd:YVO) emitting at 1064 nm, and Yttrium Lithium Fluoride (Nd:YLF), emitting at both 1053 nm (σ) and 1047 nm (π), are most commonly used [12–14]. Recently grown crystals, such as Lutetium Aluminum Garnet (Nd:LuAG), have also garnered interest for potential new applications, especially for the generation of Q-switched pulses with saturable absorbers [15].

Emissions at 1 µm are favored for efficient high-power lasers due to their greater emission cross-section. Emissions at 1.3 µm can be particularly advantageous when Raman-shifted, as their proximity to the 1.4 µm region makes them suitable for lower-cost eye-safe lasers and applications such as free space communications [16,17].

check for updates

Citation: Prado, F.M.; Franco, T.J.; Wetter, N.U. Efficient Trichromatic Nd:YLF Laser Emitting at 1047 nm, 1053 nm and 1314 nm. *Photonics* **2023**, *10*, 1146. https://doi.org/10.3390/photonics10101146

Received: 20 September 2023
Revised: 5 October 2023
Accepted: 9 October 2023
Published: 12 October 2023

While Nd:YVO and Nd:YAG exhibit higher emission cross-sections compared to the Nd:YLF, they are more susceptible to thermal effects and have shorter lifetimes. Nd:YLF, in contrast, boasts twice the upper-state lifetime of Nd:YAG and nine times that of Nd:YVO, making it an excellent choice for high-power and Q-Switched operations, especially in a side-pumping configuration for a better pump-power density distribution, reduced thermal lensing, and, consequently, greater output power [18,19]. Additionally, Nd:YLF emits at 1.31 µm, distinguishing it from Nd:YAG and Nd:YVO, which emit at around 1.34 µm, making it suitable, for example, as a local oscillator for the optical atomic calcium clock [20].

The double-wavelength emission of an Nd:YLF laser at the 1.05 µm and 1.31 µm regions was first demonstrated in 1983 [21]. However, its lamp-based pumping scheme significantly restrained efficiency. Diode-pumping overcomes this issue due to the narrow emission bandwidth of common diode lasers (<3 nm), and it is further enhanced by the use of technologies, such as volume Bragg gratings (VBG), for an even narrower emission (<0.5 nm) [22]. In 2001, Damzen et al. achieved a 75% slope efficiency and 64% conversion efficiency with diode-pumped Nd:YVO lasers in grazing-incidence single-bounce resonators. In this configuration, the laser beam undergoes a total internal reflection (TIR) at the crystal's pump face, exposing the intracavity beam's peak intensity to the area of the highest population inversion. These results were essential to establish this cavity design as an excellent alternative to highly efficient side-pumped configurations [23,24]. Recently, single-bounce resonators yielded the record-breaking slope efficiency of 68% for an Nd:YLF diode-pumped at 797 nm, although it has failed to attain a diffraction-limited output beam [25,26]. An intriguing strategy to balance efficiency and high-beam quality in these side-pumped resonators involves the incorporation of a third folding mirror within the cavity. This addition results in two, close-to-parallel laser beams undergoing both total internal reflection at the pump face of the crystal. Controlling the distance between these laser beams within the crystal diminishes the oscillation of higher-order modes, leading to a TEM_{00} output beam. This approach has been named the Double-Beam Mode Controlling Cavity (DBMC) [22,27]. It has been effectively implemented for laser emissions at 1053 nm and 1314 nm. At 1053 nm, this approach achieved a slope efficiency of 65% with TEM_{00} emission [22], while at 1314 nm, with its smaller cross-section, slope efficiencies of 54% and optical-to-optical efficiencies of 34% have been achieved with 792 nm pumping [28].

Single-bounce resonators can achieve diffraction-limited beam quality alongside remarkable efficiency values. In 2022, a side-pumped Nd:YLF laser achieved a near-quantum defect slope efficiency of 78% by directly pumping at the 863 nm wavelength. A plane-plane resonator was employed to reconcile this efficiency achievement with the desired TEM_{00} laser beam, incorporating intracavity cylindrical lenses to mitigate diffraction losses at the crystal's borders [29,30]. These single-bounce cavities are especially interesting for passively Q-switching laser applications. Their inherent simplicity aligns seamlessly with the ease of integrating a saturable absorber in the laser cavity. Furthermore, their compact nature facilitates the generation of shorter pulses without compromising energy capabilities, favoring higher peak power emissions. Recent work in 2023 showcased a Cr:YAG/Nd:YLF laser within a compact single-bounce cavity, achieving a peak power of 46 MW coupled with a pulse energy of 41 mJ. Notably, this configuration set a new benchmark for energy per pulse in passively Q-switched Nd:YLF lasers and demonstrated Q-switched dual-wavelength laser beams at 1047 nm and 1053 nm wavelengths [31].

The importance of efficient triple-wavelength emission lies in its potential to open doors to a wider array of laser applications, particularly in the generation of diverse wavelengths through phenomena such as second harmonic generation (SHG), sum- and difference frequency generation (SFG and DFG). This capability not only enriches the versatility of these lasers, but also expands their utility across various fields. A diverse range of Nd^{3+}-doped lasers have demonstrated the ability to emit triple-wavelength (multichromatic) emissions, with Nd:YGG emitting at 1062 + 1060 + 1058 nm [32], Nd:SYSO emitting at 1075 + 1076 + 1078 nm [33], Nd:YVO emitting at 1062 + 1064 + 1066 nm [34], and Nd:YAG with emissions of 1064 + 1319 + 1338 nm or even at 469 + 471 + 473 nm via frequency

doubling and sum-frequency mixing [35,36]. So far, however, Nd:YLF lasers have only presented double-wavelength emission, such as 1314 + 1321 nm [37], 1047 + 1053 nm [38], and 1047 + 1314 nm [21], presenting trichromatic emission only through the use of nonlinear effects.

To the best of our knowledge, this work demonstrates the first fundamental, triple-wavelength emission of a Nd:YLF crystal. The presented laser displays efficient multichromatic emissions at combinations of 1047 nm, 1053 nm, and 1314 nm. Each wavelength operation can be selected by simple cavity alignment, allowing for a single, double, or triple-wavelength emission. This design reached efficiencies above 31% for all wavelength operations, achieving record values for slope- and optical-to-optical efficiency at 1314 nm with 797 nm pumping.

2. Materials and Methods

A VBG-equipped 12-bar diode stack (Northrop Grumman, St. Charles, MO, USA), with 1544.8 ± 8.8 W peak power, was employed to side-pump a 13 × 13 × 3 mm^3, a-cut, Nd:YLF crystal (Crystech, Qingdao, China), with 1 mol% Nd^{3+} doping. The pumping duty cycle of 0.17% (350 µs; 5 Hz) was set by the manufacturer to maintain the 797 nm emission line at a measured width of 0.92 ± 0.03 nm at Full Width at Half Maximum (FWHM). The pump diode's emission was focused by a doublet lens (D), with f = 30 mm, to guarantee good spatial overlap between pump- and laser beams. A half-wave plate (HP) was employed to set the polarization of the pump diode to be parallel to the c-axis of the crystal, improving absorption.

The resonator configuration used a total internal reflection at the pump facet of the crystal to expose the center of the TEM_{00} mode (the peak intensity of the intracavity beam) to the area of highest population inversion. A Brewster's angle of incidence ($\Theta_B = 55.4°$ for the σ-transition) was employed at the uncoated lateral faces of the crystal for the intracavity beam to achieve wavelength emission at 1314 nm (σ-polarized) and to reduce Fresnel reflection losses.

Due to its significantly lower emission cross-section at 1.31 µm, laser emission requires the employment of mirrors with high transmittance at 1.05 µm. Therefore, a plane output coupler (M1), with transmissions of $T_{-1.31\ \mu m}$ = 10% and $T_{-1.05\ \mu m}$ = 75%, and a highly reflective (HR) concave mirror at 1.31 µm (M2), with a radius of curvatures (ROC) of 8 m and $T_{-1.05\ \mu m}$ = 92%, were used to achieve emission of 1314 nm. In this two-mirror configuration, the reflection of M1 and M2 in the 1.05 µm region is still sufficient for 1047 nm oscillation when at least one of the laser mirrors is slightly misaligned to impede 1314 nm oscillation. The misalignment effectively diminishes reflectivity at 1314 nm, increasing the resonator's tendency to oscillate at the 1.05 µm region due to its larger emission cross-section, as shown in Table 1.

Table 1. Nd:YLF stimulated emissions cross sections at 1047, 1053, 1321, and 1314 nm [18,39].

Nd:YLF	$^4F_{3/2} \rightarrow {}^4I_{11/2}$		$^4F_{3/2} \rightarrow {}^4I_{13/2}$	
	1047 nm (π)	**1053 nm (σ)**	**1321 nm (π)**	**1314 nm (σ)**
σ_e (10^{-19} cm^2)	1.8	1.2	0.27	0.33

The low reflectivity of both mirrors at 1.05 µm, together with the lower emission cross-section of the 1053 nm wavelength, favors the oscillation of the π-polarized wavelength of 1047 nm, despite the use of a Brewster angle of incidence for the σ-transition. Therefore, to achieve 1053 nm wavelength emission, a 1.05 µm HR plane mirror (M3) was added behind the M2 mirror, as shown in Figure 1A.

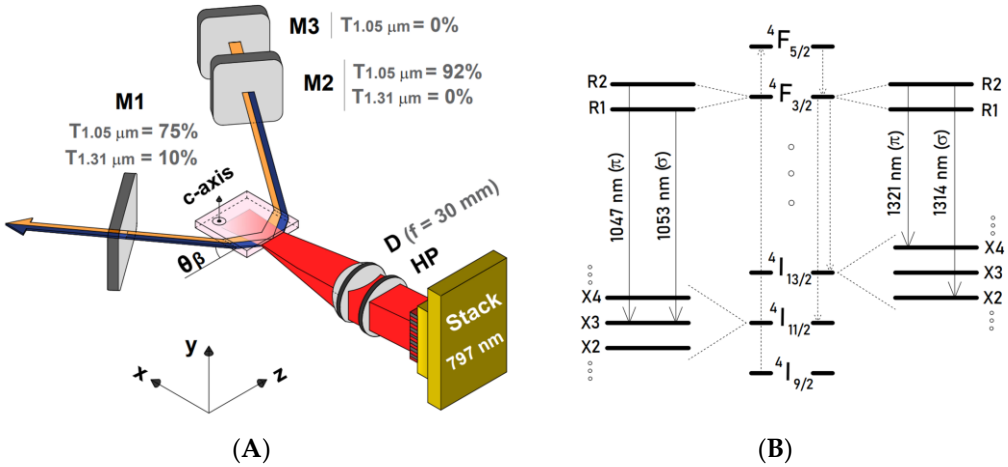

Figure 1. (**A**): Single-bounce resonator configuration. M1, M2, and M3 are laser mirrors; D is a doublet with a 30 mm focal distance; HP is a half-wave plate. (**B**): Diagram of the relevant energy transitions in Nd:YLF [40,41].

Figure 2 presents the transmittance spectrum, measured by a Varian CARY® 5000 spectrometer (Agilent Technologies, Santa Clara, CA, USA), of all three mirrors utilized in the laser resonator.

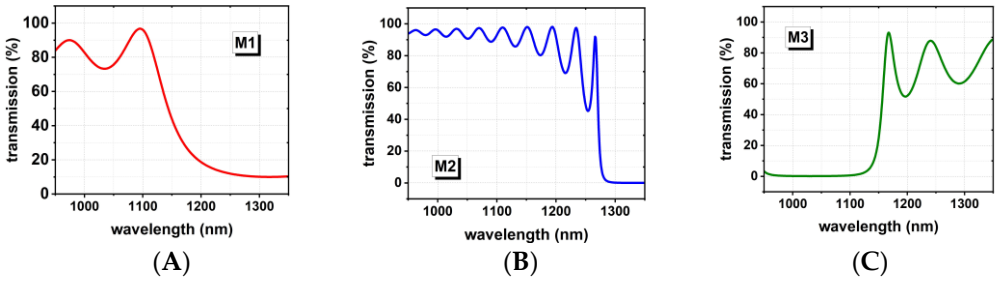

Figure 2. Spectrum of laser mirrors (950 nm to 1350 nm). (**A**): Transmission of M1. (**B**): Transmission of M2. (**C**): Transmission of M3.

The cavity length between M1 and M2 was set to 140 mm, resulting in a (simulated; LASCAD v. 3.6) mode spot radius inside the crystal of 1983 μm × 1148 μm in the horizontal and vertical directions, respectively, using the M^2 beam quality factor, shown in Figure 6 (measured for the σ–transition of 1314 nm. The cavity length between M1 and M3 was set to 180 mm, resulting in a spot size (radius) of 1931 μm × 1275 μm in the horizontal and vertical directions, respectively. It should be noted that the larger horizontal dimension is caused by two factors, the Brewster angle of incidence at the crystal's side facets and the larger M^2 beam quality factor in the horizontal direction. With a measured pump spot size of 2100 ± 250 μm × 145 ± 30 μm, we guarantee good spatial overlap by focusing the pump light into a smaller spot size at the crystal's pump surface than the area of the TIR of the simulated laser mode, especially in the vertical direction. We remark that because of Brewster angle of incidence of the laser mode at the TIR surface inside the crystal, the beam size in the pump direction is an additional n times larger (n being the refractive index of the σ–transition) than the mode spot size inside the crystal. Therefore, the overlap integral benefits from the geometry of this set-up is responsible for an n^2 -times larger laser beam mode in the pump direction. Specifically in the above case, the $1/e^2$ mode size in the pump direction is 5.75 mm for the M1–M2 cavity.

The spectral overlap was calculated with a MatLab script in which, in the first step, convolutes the emission curve of the pump diode with the absorption spectrum of the Nd:YLF crystal with 1% doping, shown in Figure 3A,B, respectively. As a result, the effective absorption coefficient decreases non-exponentially as a function of the absorption

depth inside the crystal, because the diode's frequencies closest to its emission peak are more efficiently absorbed by the crystal's narrow absorption peak if both spectra overlap perfectly, when compared to frequencies farther away from the diode's emission peak. Figure 3C displays the effective absorption as a function of the pump depth. The absorption at 5.75 mm is higher than 97%. The effective absorption coefficient needs to be considered in order to calculate the overall overlap efficiency below (Equation (1)).

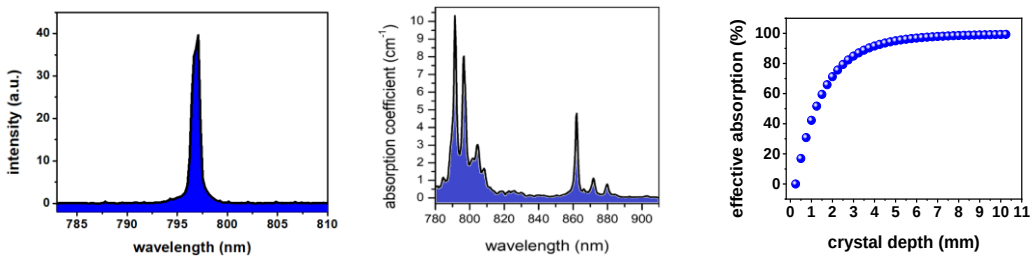

(**A**) (**B**) (**C**)

Figure 3. (**A**): Emission spectrum of 797 nm diode stack, measured by a HR2000 spectrometer (OceanInsight, Orlando, FL, USA) with 0.24 nm resolution at FWHM; (**B**): Absorption spectrum of Nd:YLF, measured by a Varian CARY® 5000 spectrometer. (**C**): Effective absorption in function of the pump depth.

In agreement with the theory of Kubodera et al. [42], the total overlap efficiency of the system can be defined as the integral of the spatial, normalized population inversion saturated by the oscillating field, also called remaining inversion, divided by non-saturated inversion.

$$\iiint \frac{r_0(x,y,z)}{1+\sum_j S_j s_{0j}(x,y,z)/I_0} dv \Big/ \iiint r_0(x,y,z)dv \quad (1)$$

where dv is integrated over the pump volume, I_0 is the saturation intensity, S_j the photon number in TEM mode j, s_{0j} and r_0 the normalized distribution function of mode j and the pump mode, respectively. The Matlab script calculates which ressonator mode j enters oscillation first, under the condition of a specific pump distribution. From there on it calculates, for each pump power, the denominator in Equation (1) for the sum of all oscillating modes $\boldsymbol{j}$ and checks if another additional mode $\boldsymbol{i}$ can oscillate (reach threshold) at the same pump power R. The Matlab code then resolves the system of $\boldsymbol{i}$ non-linear equations and calculates the values of S_j for each mode, which is proportional to the fractional output power of each mode. The calculated resultant overlap efficiency is 98.3% for the 1314 nm transition.

Wavelength Selection

To comprehend the mechanism of selection of each wavelength, we first examine a resonator equipped with only two laser mirrors, M1 and M2. When both mirrors are precisely aligned, the laser cavity is optimized for single-wavelength operation at 1314 nm. This occurs due to both mirrors having high transmittance in the 1 µm range and optimal reflectivity for 1314 nm. Since the $^4F_{3/2} \rightarrow {}^4I_{11/2}$ transition has a much larger emission cross-section compared to the $^4F_{3/2} \rightarrow {}^4I_{13/2}$ transition, emission at 1.05 µm is achieved by intentionally disturbing the alignment of M2 for 1314 nm emission. This misalignment disrupts the conditions for 1314 nm emission, reducing the competition from 1314 nm and allowing the emergence of the 1047 nm wavelength. The transition from 1314 nm to 1047 nm, or vice versa, occurs gradually as we reduce alignment for the 1314 nm wavelength. As a result, we can achieve any combination of both wavelengths simultaneously just by controlling the alignment of the cavity's mirrors. Mirror M3 assumes a pivotal role by increasing reflectivity at 1.05 µm, thereby enabling the emission of the 1053 nm wavelength and also enhancing efficiency at the 1.047 µm transition. By adjusting the alignment of M3 and considering the 1047 nm losses induced by the Brewster angle of incidence, which causes an 8% reflection loss per surface for this wavelength, we can facilitate the emission

of either 1047 nm or 1053 nm, or even a combination of both simultaneously. Therefore, triple wavelength emission of 1047 nm, 1053 nm and 1314 nm is achieved by using main alignment of M3 for controlling the relative emission intensity of 1047 nm and 1053 nm while M2 controls the 1.3 μm emission.

3. Results and Discussion

Figure 4 shows the spectrum of the laser emitting in single-wavelength operation at 1047 nm, 1053 nm, and 1314 nm in the dual-wavelength regime at 1047 nm and 1053 nm, 1047 nm and 1314 nm, 1053 nm and 1314 nm, and during triple-wavelength emission of 1047 nm, 1053 nm and 1314 nm. The 1047 nm and 1053 nm emissions were measured with a fiber-coupled (50 μm fiber) high-resolution spectrometer (HR2000; Ocean Optics Inc., Orlando, FL, USA, 0.24 nm resolution at FWHM), yielding an emission line width at FWHM of 0.27 ± 0.1 nm and 0.38 ± 0.1 nm for 1047 nm and 1053 nm, respectively. The emission at 1314 nm was measured by a fiber-coupled InGaAs spectrometer (NIR quest; Ocean Optics Inc., 3.3 ± 0.2 nm FWHM resolution) using a 10 μm fiber.

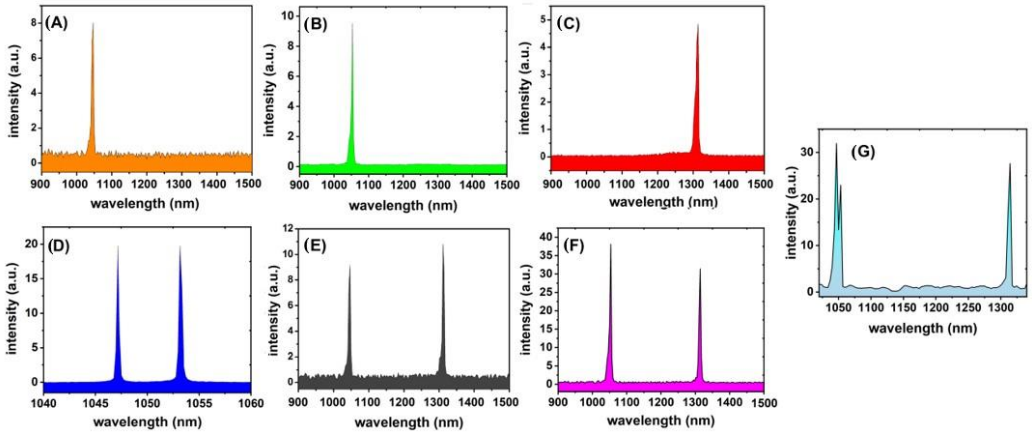

Figure 4. Emission spectra of the Nd:YLF laser. (**A**): 1047 nm emission. (**B**): 1053 nm. (**C**): 1314 nm. (**D**): simultaneous emission of 1047 nm and 1053 nm. (**E**): 1047 nm and 1314 nm. (**F**): 1053 nm and 1314 nm. (**G**): 1047 nm, 1053 nm, and 1314 nm (resolution of 3.3 ± 0.2 nm).

Even at high-pump powers the laser did not present thermal lensing or any special cooling requirements due to the low duty cycle; the maximum average pump power was of the order of 2.7 W. Figure 5 shows the peak output power vs. the incident pump power after the 3.6% Fresnel losses at the pump face of the crystal for each of the three emission regimes of the laser cavity.

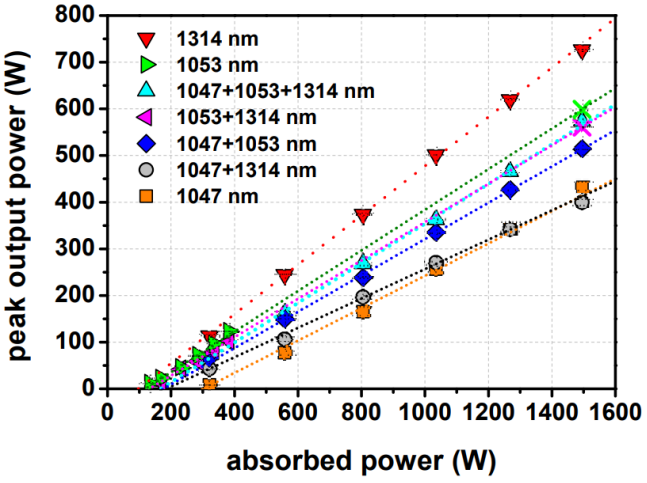

Figure 5. Peak output power vs. incident power for the emissions of: 1314 nm, 1053 nm, 1047 + 1053 + 1314 nm, 1053 + 1314 nm, 1047 + 1053 nm, 1047 + 1314 nm, and 1047 nm.

A slope efficiency of 52.8 ± 0.7% and an optical-to-optical efficiency of 48.6 ± 0.3% were achieved for the single wavelength emission at 1314 nm. To the best of our knowledge, this represents the highest optical-to-optical efficiency achieved at 1314 nm to date and the best slope efficiency for 797 nm pumping. When optimized for 1047 nm or 1053 nm emission, measured slope efficiencies were 34.7 ± 0.9% and 43.5 ± 0.5%, respectively. Dual-wavelength emission at 1047 + 1053 nm or at 1047 + 1314 nm resulted in slope efficiencies of 38.9 ± 0.5% and 31.5 ± 0.5%, respectively, while 1053 + 1314 nm emission yielded a value of 41.1 ± 0.4%. Finally, the triple-wavelength emission of 1047 + 1053 + 1314 nm presented a slope efficiency of 42.5 ± 0.6% and an optical-to-optical efficiency of 38.4 ± 0.3. Table 2 presents the results of peak output power, pulse width, slope efficiency, and optical efficiency for each wavelength combination.

Table 2. Measured Nd:YLF monochromatic, bichromatic, and trichromatic laser results (* optical efficiency calculated from slope efficiency).

Nd:YLF Laser	Laser Emission Regime						
	1314 nm	**1047 nm**	**1053 nm**	**1047 + 1053 nm**	**1047 + 1314 nm**	**1053 + 1314 nm**	**1047 + 1053 + 1314 nm**
Peak Output Power (W)	726 ± 3	434 ± 11	124 ± 1	514 ± 4	400 ± 9	102 ± 1	574 ± 3
Pulse width (μs)	342 ± 0.1	315 ± 1	338 ± 2	332 ± 0.2	314 ± 1	335 ± 1	331 ± 0.2
Slope efficiency (%)	53 ± 1	35 ± 1	43 ± 0.5	39 ± 0.5	31 ± 0.5	41 ± 0.4	42 ± 1
Optical efficiency (%)	49 ± 0.3	29 ± 1	40 ± 0.2 *	34 ± 0.3	27 ± 1	37.5 ± 0.2 *	38 ± 0.3

The provided peak output power and pulse width values include standard deviation (SD) errors. Slope and optical efficiency values incorporate errors from curve fitting and uncertainty propagation, respectively. The relatively low standard deviation (SD) values in the peak output power demonstrate the stability and minimal power fluctuation between different laser operation modes.

The unoptimized mirror reflectivity of M2 at 1047 nm and 1053 nm limits the efficiency values achieved at these wavelengths. One could increase their efficiencies simply by exchanging the order of placement of M2 and M3, but at the cost of the high-efficiency emission at 1314 nm.

The M^2 value was measured by the knife edge technique using 10/90 clip levels and a correction factor of 1.561 to calculate the beam waist at $1/e^2$ [43,44]. Figure 6 shows the measured and corrected beam waist of the 1314 nm emission as a function of the distance from a spherical focusing lens with f = 40 mm. A similar curve fit was used to determine the M^2 for wavelengths at the 1.05 μm region.

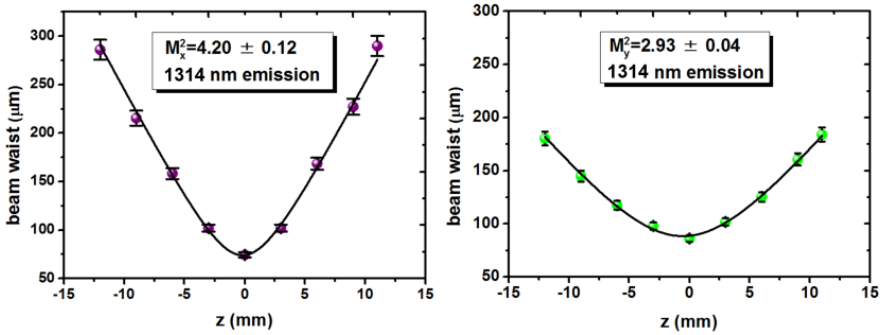

Figure 6. Beam waist curve fit made by utilizing the Knife Edge Technique in the x in y axis, respectively.

These M^2 measurements were made for each wavelength during simultaneous triple wavelength operation with near equal amplitude. To separate the beams, a combination of a high-pass filter at 1.3 μm (Thorlabs, FELO1300), a HR mirror for 1.3 μm with high transmission at 1.05 μm, and a polarizer to isolate the emissions of the 1.05 μm emission were employed. For each wavelength, horizontal and vertical values were measured, all of which are shown in Table 3.

Table 3. M^2 values 1047 nm, 1053 nm, and 1314 nm wavelengths.

Wavelength	M^2	
	x	y
1314 nm	4.2 ± 0.1	2.93 ± 0.4
1047 nm	2.4 ± 0.3	2.2 ± 0.4
1053 nm	4.1 ± 0.2	2.4 ± 0.1

Compared to other simple single-bounce, diode-pumped Nd:YLF lasers operating in the 1 μm region, the achieved M_x^2 values of 2.4 at 1047 nm and 4.1 at 1053 nm perform well [25,31]. The M^2 values obtained for 1314 nm emission fare well when compared with similar compact cavities, especially considering the absence of any configuration for beam quality improvements, such as a DBMC or a larger resonator with intracavity cylindrical lenses [28].

The advantage of achieving efficient triple-wavelength emission, without the need for additional optical elements within the cavity, holds great value in the development of compact, cost-effective, and versatile lasers suitable for a wide range of applications. This is particularly evident in its application within χ^2 nonlinear phenomena, including Second Harmonic Generation, Sum Frequency Generation, and Difference Frequency Generation. These nonlinear processes allow for wavelength transformations, leading to a diverse range of multichromatic visible- and near-infrared (NIR) radiation, producing frequencies as low as 1.6 THz, using DFG for the 1047 + 1053 nm emission, and extend to 58 THz by employing SFG for the 1047 + 1314 nm emission, for example. Furthermore, although considerably more challenging, nonlinear transformations with triple-wavelength emission have the potential to generate radiation up to the 800 THz range when combined with SFG.

4. Conclusions

Simultaneous triple-wavelength emission at 1047 + 1053 + 1314 nm of a side-pumped Nd:YLF laser in a simple and compact cavity is presented for the first time. The wavelength selection of single, double, and triple-wavelength operation was made exclusively by cavity alignment and delivered a record slope and optical-to-optical efficiency of 53% and 49%, respectively, when optimized for the single 1314 nm emission, representing the highest efficiency achieved at this wavelength while pumped at 797 nm. Meanwhile, other wavelength operations remained, in all cases, above 31% of slope efficiency.

The beam qualities of all three wavelengths fare well when compared with related works. However, they could be further improved by employing techniques such as double-beam mode controlling the cavity or increasing the crystal's laser mode size by applying cylindrical intracavity lenses. The resonator shows good promise for passive Q-switch applications, especially with broadband saturable absorbers such as V^{3+}:YAG. The high-peak power multichromatic emission could facilitate the operation of a compact, multi-wavelength laser in the visible NIR and infrared by using non-linear processes such as SHG, DFG, and SFG.

Author Contributions: Conceptualization, F.M.P., T.J.F. and N.U.W.; methodology, F.M.P., N.U.W. and T.J.F.; validation, F.M.P., N.U.W. and T.J.F.; formal analysis, N.U.W., F.M.P. and T.J.F.; investigation, F.M.P. and T.J.F.; resources, N.U.W.; data curation, F.M.P.; writing—original draft preparation, T.J.F.; writing—review and editing, F.M.P. and N.U.W.; visualization, F.M.P.; supervision, N.U.W.; project administration, N.U.W.; funding acquisition, N.U.W. All authors have read and agreed to the published version of the manuscript.

Funding: This research was funded by the São Paulo State Research Support Foundation (FAPESP), grant numbers 2022/15276-0, 2012/11437-8; the Brazilian National Council for Scientific and Technological Development (CNPq), grant numbers 3085262021-0, 2014-6 465763.

Institutional Review Board Statement: Not applicable.

Informed Consent Statement: Not applicable.

Data Availability Statement: Data underlying the results presented in this paper are not publicly available but may be obtained from the authors upon reasonable request.

Conflicts of Interest: The authors declare no conflict of interest.

References

1. Pavel, N. Simultaneous Dual-Wavelength Emission at 0.90 and 1.06 μm in Nd-Doped Laser Crystals. *Laser Phys.* **2010**, *20*, 215–221. [CrossRef]
2. Walsh, B.M. Dual Wavelength Lasers. *Laser Phys.* **2010**, *20*, 622–634. [CrossRef]
3. Hussain, T.; Gondal, M.A. Laser Induced Breakdown Spectroscopy (LIBS) as a Rapid Tool for Material Analysis. *J. Phys. Conf. Ser.* **2013**, *439*, 012050. [CrossRef]
4. Basler, C.; Brandenburg, A.; Michalik, K.; Mory, D. Comparison of Laser Pulse Duration for the Spatially Resolved Measurement of Coating Thickness with Laser-Induced Breakdown Spectroscopy. *Sensors* **2019**, *19*, 4133. [CrossRef]
5. Basler, C.; Kappeler, M.; Carl, D. Depth-Resolved Elemental Analysis on Moving Electrode Foils with Laser-Induced Breakdown Spectroscopy. *Sensors* **2023**, *23*, 1082. [CrossRef] [PubMed]
6. Ahmad, H.; Muhammad, F.D.; Pua, C.H.; Thambiratnam, K. Dual-Wavelength Fiber Lasers for the Optical Generation of Microwave and Terahertz Radiation. *IEEE J. Sel. Top. Quantum Electron.* **2014**, *20*, 166–173. [CrossRef]
7. Angeluts, A.A.; Bezotosnyi, V.V.; Cheshev, E.A.; Goltsman, G.N.; Finkel, M.I.; Seliverstov, S.V.; Evdokimov, M.N.; Gorbunkov, M.V.; Kitaeva, G.K.; Koromyslov, A.L. Compact 1.64 THz Source Based on a Dual-Wavelength Diode End-Pumped Nd:YLF Laser with a Nearly Semiconfocal Cavity. *Laser Phys. Lett.* **2014**, *11*, 015004. [CrossRef]
8. Polyakov, V.M.; Vitkin, V.V.; Lychagin, D.I.; Krylov, A.A.; Buchenkov, V.A.; Kashcheev, S.V. Compact Q-Switched High Repetition Rate Nd:YLF Laser with 100 MJ Pulse Energy for Airborne Lidars. In Proceedings of the 2014 International Conference Laser Optics, St. Petersburg, Russia, 30 June–4 July 2014; IEEE Computer Society: Piscataway, NJ, USA, 2014.
9. Geskus, D.; Jakutis-Neto, J.; Pask, H.M.; Wetter, N.U. Intracavity Frequency Converted Raman Laser Producing 10 Deep Blue to Cyan Emission Lines with up to 094 W Output Power. *Opt. Lett.* **2014**, *39*, 6799–6802. [CrossRef] [PubMed]
10. Ferreira, M.S.; Wetter, N.U. Diode-Side-Pumped, Intracavity Nd:YLF/KGW/LBO Raman Laser at 573 Nm for Retinal Photocoagulation. *Opt. Lett.* **2021**, *46*, 508–511. [CrossRef]
11. Geskus, D.; Neto, J.J.; Reijn, S.-M.; Pask, H.M.; Wetter, N.U. Quasi-Continuous Wave Raman Lasers at 990 and 976 Nm Based on a Three-Level Nd:YLF Laser. *Opt. Lett.* **2014**, *39*, 2982–2985. [CrossRef] [PubMed]
12. Demirbas, U.; Uecker, R.; Fujimoto, J.G.; Leitenstorfer, A. Multicolor Lasers Using Birefringent Filters: Experimental Demonstration with Cr:Nd:GSGG and Cr:LiSAF. *Opt. Express* **2017**, *25*, 2594–2607. [CrossRef]
13. Wetter, N.U.; Camargo, F.A.; Sousa, E.C. Mode-Controlling in a 7.5 cm Long, Transversally Pumped, High Power Nd:YVO_4 Laser. *J. Opt. A Pure Appl. Opt.* **2008**, *10*, 104012. [CrossRef]
14. Deana, A.M.; Ranieri, I.M.; Baldochi, S.L.; Wetter, N.U. Compact, Diode-Side-Pumped and Q-Switched Nd:$YLiF_4$ Laser Cavity Operating at 1053 Nm with Diffraction Limited Beam Quality. *Appl. Phys. B* **2012**, *106*, 877–880. [CrossRef]
15. Zhang, G.; Liu, T.; Shen, Y.; Zhao, C.; Huang, B.; Kang, Z.; Qin, G.; Liu, Q.; Fu, X. 516 mW, nanosecond Nd:LuAG laser Q-switched by gold nanorods. *Chin. Opt. Lett.* **2018**, *16*, 030011. [CrossRef]
16. Jahid, A.; Alsharif, M.H.; Hall, T.J. A Contemporary Survey on Free Space Optical Communication: Potentials, Technical Challenges, Recent Advances and Research Direction. *J. Netw. Comput. Appl.* **2022**, *200*, 103311. [CrossRef]
17. Kores, C.C.; Jakutis-Neto, J.; Geskus, D.; Pask, H.M.; Wetter, N.U. Diode-Side-Pumped Continuous Wave Nd^{3+}:YVO_4 Self-Raman Laser at 1176 nm. *Opt. Lett.* **2015**, *40*, 3524–3527. [CrossRef]
18. Czeranowsky, C. *Resonatorinterne Frequenzverdopplung von Diodengepumpten Neodym-Lasern Mit Hohen Ausgangsleistungen Im Blauen Spektralbereich*; University of Hamburg: Hamburg, Germany, 2002.
19. Koechner, W.; Bass, M. *Solid-State Lasers: Advanced Texts in Physics*; Springer: New York, NY, USA, 2003; ISBN 978-0-387-95590-2.
20. Nunez Portela, M.; Wetter, N.U.; Zondy, J.J.; Cruz, F.C. A Single-Frequency, Diode-Pumped Nd:YLF Laser at 657 Nm: A Frequency and Intensity Noise Comparison with an Extended Cavity Diode Laser. *Laser Phys.* **2013**, *23*, 025801. [CrossRef]
21. Vollmar, W.; Knights, M.G.; Rines, G.A.; Mccarthy, J.C.; Chicklis, E.P. Five-Color Nd:YLF Laser. In *Proceedings of the Conference on Lasers and Electro-Optics, Baltimore, MD, USA, 17–20 May 1983*; OSA: Washington, DC, USA, 1983; p. THM2.
22. Wetter, N.U.; Deana, A.M. Influence of Pump Bandwidth on the Efficiency of Side-Pumped, Double-Beam Mode-Controlled Lasers: Establishing a New Record for Nd:$YLiF_4$ Lasers Using VBG. *Opt. Express* **2015**, *23*, 9379–9387. [CrossRef] [PubMed]
23. Damzen, M.J.; Trew, M.; Crofts, G.J.; Rosas, E. 22.5W Continuous-Wave Nd:YVO_4 Grazing-Incidence Laser with 62% Conversion Efficiency. In *Proceedings of the Advanced Solid-State Lasers, Seattle, WA, USA, 28–31 January 2001*; OSA: Washington, DC, USA, 2001; p. MD4.
24. Damzen, M.J.; Trew, M.; Rosas, E.; Crofts, G.J. Continuous-Wave Nd:YVO_4 Grazing-Incidence Laser with 22.5 W Output Power and 64% Conversion Efficiency. *Opt. Commun.* **2001**, *196*, 237–241. [CrossRef]
25. Prado, F.M.; Franco, T.J.; Vieira, T.A.; Wetter, N.U. High Power Nd:YLF Four-Level Lasers with 68% Slope Efficiency. *Appl. Opt.* **2023**, *62*, C49–C52. [CrossRef]

26. Prado, F.; Wetter, N.U. Nd:YLF Laser Pumped at 797 Nm with 68% Slope Efficiency. In Proceedings of the Solid State Lasers XXXI: Technology and Devices, San Francisco, CA, USA, 22–27 January 2022; Clarkson, W.A., Shori, R.K., Eds.; SPIE: Bellingham, WA, USA, 2022; p. 18.
27. Wetter, N.U.; Deana, A.M. Diode-Side-Pumped Nd:$YLiF_4$ Laser Emitting at 1053 nm with 53.6% Optical Efficiency and Diffraction-Limited Beam Quality. *Laser Phys. Lett.* **2013**, *10*, 035807. [CrossRef]
28. Deana, A.M.; Lopez, M.A.P.A.; Wetter, N.U. Diode-Side-Pumped Nd:YLF Laser Emitting at 1313 Nm Based on DBMC Technology. *Opt. Lett.* **2013**, *38*, 4088–4091. [CrossRef]
29. Vieira, T.A.; Prado, F.M.; Wetter, N.U. Nd:YLF Laser at 1053 Nm Diode Side Pumped at 863 nm with a near Quantum-Defect Slope Efficiency. *Opt. Laser Technol.* **2022**, *149*, 107818. [CrossRef]
30. Vieira, T.A.; Prado, F.M.; Wetter, N.U. Near Quantum Limited Slope Efficiency Nd:YLF4 Laser. In Proceedings of the Laser Congress 2021 (ASSL, LAC), Washington, DC, USA, 3–7 October 2021; Optica Publishing Group: Washington, DC, USA, 2021; p. AW3A.6.
31. Prado, F.M.; Franco, T.J.; Wetter, N.U. Sub-Nanosecond, 41 MJ Pulse Energy, Passively Q-Switched Nd:YLF Laser. *Opt. Laser Technol.* **2023**, *162*, 109257. [CrossRef]
32. Yu, H.; Wu, K.; Yao, B.; Zhang, H.; Wang, Z.; Wang, J.; Zhang, X.; Jiang, M. Efficient Triwavelength Laser with a Nd:YGG Garnet Crystal. *Opt. Lett.* **2010**, *35*, 1801–1803. [CrossRef] [PubMed]
33. Hou, J.; Zheng, L.H.; He, J.L.; Xu, J.; Zhang, B.T.; Wang, Z.W.; Lou, F.; Wang, R.H.; Liu, X.M. A Tri-Wavelength Synchronous Mode-Locked Nd:SYSO Laser with a Semiconductor Saturable Absorber Mirror. *Laser Phys. Lett.* **2014**, *11*, 035803. [CrossRef]
34. Lin, Z.; Wang, Y.; Xu, B.; Xu, H.; Cai, Z. Diode-Pumped Simultaneous Multi-Wavelength Linearly Polarized Nd:YVO_4 Laser at 1062, 1064 and 1066 nm. *Laser Phys.* **2016**, *26*, 015801. [CrossRef]
35. Chen, L.; Wang, Z.; Liu, H.; Zhuang, S.; Yu, H.; Guo, L.; Lan, R.; Wang, J.; Xu, X. Continuous-Wave Tri-Wavelength Operation at 1064, 1319 and 1338 Nm of LD End-Pumped Nd:YAG Ceramic Laser. *Opt. Express* **2010**, *18*, 22167–22173. [CrossRef]
36. Xu, B.; Camy, P.; Doualan, J.-L.; Braud, A.; Cai, Z.; Balembois, F.; Moncorgé, R. Frequency Doubling and Sum-Frequency Mixing Operation at 4692, 471, and 473 Nm in Nd:YAG. *J. Opt. Soc. Am. B* **2012**, *29*, 346–350. [CrossRef]
37. Tu, Z.; Dai, S.; Zhu, S.; Yin, H.; Li, Z.; Ji, E.; Chen, Z. Efficient High-Power Orthogonally-Polarized Dual-Wavelength Nd:YLF Laser at 1314 and 1321 nm. *Opt. Express* **2019**, *27*, 32949–32957. [CrossRef] [PubMed]
38. Cho, C.Y.; Huang, T.L.; Wen, S.M.; Huang, Y.J.; Huang, K.F.; Chen, Y.F. Nd:YLF Laser at Cryogenic Temperature with Orthogonally Polarized Simultaneous Emission at 1047 nm and 1053 nm. *Opt. Express* **2014**, *22*, 25318–25323. [CrossRef]
39. Turri, G.; Webster, S.; Bass, M.; Toncelli, A. Temperature-Dependent Stimulated Emission Cross-Section in Nd^{3+}:YLF Crystal. *Materials* **2021**, *14*, 431. [CrossRef] [PubMed]
40. Xu, S.; Gao, S. A New Wavelength Laser at 1370 nm Generated by Nd:YLF Crystal. *Mater. Lett.* **2016**, *183*, 451–453. [CrossRef]
41. Pollnau, M.; Hardman, P.J.; Kern, M.A.; Clarkson, W.A.; Hanna, D.C. Upconversion-Induced Heat Generation and Thermal Lensing in Nd:YLF and Nd:YAG. *Phys. Rev. B* **1998**, *58*, 16076–16092. [CrossRef]
42. Kubodera, K.; Otsuka, K. Single-Transverse-Mode LiNdP4O12 Slab Waveguide Laser. *J. Appl. Phys.* **1979**, *50*, 653–659. [CrossRef]
43. Siegman, A.E. Choice of Clip Levels for Beam Width Measurements Using Knife-Edge Techniques. *IEEE J. Quantum Electron.* **1991**, *27*, 1098–1104. [CrossRef]
44. Siegman, A.E. How to (Maybe) Measure Laser Beam Quality. In *Proceedings of the DPSS (Diode Pumped Solid State) Lasers: Applications and Issues, Washington, DC, USA, 1–4 December 1998*; OSA: Washington, DC, USA, 1998; p. MQ1.